

**STUDY OF MALAYSIAN RARE EARTH ELEMENTS:
MINERAL CHARACTERIZATION OF MONAZITE AND
XENOTIME CONCENTRATE FROM AMANG**

NURUL FATIN NAZIRA BINTI NAZATUL DZAHIR

UNIVERSITI SAINS MALAYSIA

2022

**STUDY OF MALAYSIAN RARE EARTH ELEMENTS:
MINERAL CHARACTERIZATION OF MONAZITE AND
XENOTIME CONCENTRATE FROM AMANG**

by

NURUL FATIN NAZIRA BINTI NAZATUL DZAHIR

**A thesis submitted in fulfillment of the requirements for the degree of Bachelor's
Degree in Mineral Resources Engineering with Honours**

AUGUST 2022

ACKNOWLEDGEMENT

Bismillahirrahmanirrahim. In the name of Allah, the Most Gracious, the Most Merciful. *Alhamdulillah*, on completion of my final year project and this thesis. I would like to thank my beloved family and fiancé for their unwavering support to continually push myself to complete my final year project.

First of all, I would like to express my deepest thanks to my supportive supervisor, Dr. Zakaria Bin Endut who despite being extraordinarily busy with his duties, for the useful comments, remarks, and engagement throughout the project. He prompts inspiration, suggestions, and guidance. I attribute the level of my Bachelor's degree to his encouragement and effort because, without him, this thesis would not have been completed or written.

Instead, I offer my sincerest gratitude to my co-supervisor, Pn Khaironie Binti Mohamed Takip, and Malaysian Nuclear Agency (ANM) who has provided me with the concentrate samples for my project and supported me throughout this project. Besides that, great appreciation also goes to all the lecturers, staff, and technicians, especially Pn. Faziatun Binti Dahari, En Zul, Encik Junaidi, Encik Meor, Encik Rasyid. who assisted and supported me during my lab work. Instead, I also express my sincere gratitude to all my friends for their willingness to share their wisdom and constructive suggestions during the project.

Last but not least, I would like to express my appreciation to those who went unmentioned for their assistance and counsel. Without all the guidance and help from all the parties, I may not finish my research perfectly. May Allah bless you all. Thank you very much.

TABLE OF CONTENTS

ACKNOWLEDGEMENT	ii
TABLE OF CONTENTS	iii
LIST OF TABLES	vi
LIST OF FIGURES	vii
LIST OF SYMBOLS	x
LIST OF ABBREVIATIONS	xi
LIST OF APPENDICES	xii
ABSTRAK	xiii
ABSTRACT	xiv
CHAPTER 1 INTRODUCTION	1
1.1 Research Background	1
1.2 Problem Statements	3
1.3 Research Objectives	4
CHAPTER 2 LITERATURE REVIEW	5
2.1 Introduction.....	5
2.2 Amang.....	5
2.3 Rare Earth Elements (REEs).....	7
2.4 Monazite	9
2.5 Xenotime.....	10
2.6 Characterization of Monazite and Xenotime	11
2.6.1 Particle Size Analysis.....	11
2.6.2 Moisture content	12
2.6.3 X-Ray Fluorescence (XRF)	13
2.6.4 Micro X-Ray Fluorescence (Micro-XRF).....	14
2.6.5 X-Ray Diffraction (XRD)	15

2.6.6	Ore Microscopy	16
2.6.7	Scanning Electron Microscopy (SEM)	17
2.6.8	Scanning Electron Microscopy(SEM)/ Energy Dispersive X-Ray(EDX).....	18
2.7	Crystallography	19
2.7.1	Monazite	24
2.7.2	Xenotime	27
2.8	Summary.....	29
CHAPTER 3 METHODOLOGY.....		31
3.1	Introduction.....	31
3.2	Experimental Flowchart.....	32
3.3	Sample Preparation.....	33
3.3.1	Sampling.....	33
3.3.2	Moisture content	33
3.4	Sample Characterization	34
3.4.1	Preparation of polished sections	34
3.4.2	Particle Size Distribution.....	34
3.4.3	Elemental Composition	35
3.4.3(a)	X-Ray Fluorescence (XRF)	35
3.4.3(b)	Micro X-Ray Fluorescence (Micro-XRF)	36
3.4.4	Phase Identification.....	36
3.5	Morphology Study.....	38
3.5.1	Ore Microscopy	38
3.5.2	Scanning Electron Microscopy (SEM)	38
3.5.3	Scanning Electron Microscopy(SEM)/ Energy Dispersive X-Ray(EDX).....	39
CHAPTER 4 RESULTS AND DISCUSSION		40
4.1	Introduction.....	40

4.2	Moisture content.....	40
4.3	Particle Size Distribution	41
4.4	Visual assessment.....	48
4.5	Morphology study	49
4.5.1	Optical microscope	49
4.5.2	SEM TableTop.....	50
4.5.2(a)	Monazite	50
4.5.2(b)	Xenotime	52
4.5.3	SEM/EDX.....	54
4.5.3(a)	Monazite	54
4.5.3(b)	Xenotime	56
4.6	Elemental Composition Analysis	58
4.6.1	X-Ray Fluorescence (XRF).....	58
4.6.2	Micro X-Ray Fluorescence (Micro-XRF).....	61
4.6.2(a)	Monazite	61
4.6.2(b)	Xenotime	65
4.7	Phase Identification Analysis.....	65
4.8	Application For Industry.....	68
CHAPTER 5 CONCLUSION AND FUTURE RECOMMENDATIONS		70
5.1	Conclusion	70
5.2	Recommendations for Future Research.....	71
REFERENCES		72
APPENDICES		

LIST OF TABLES

	Page
Table 1	All of the 32 crystal system and classes with their symmetry components..... 23
Table 2	Moisture content analysis result 40
Table 3	Particle size distribution of monazite concentrate sample. 42
Table 4	Particle size distribution of xenotime concentrate sample. 42
Table 5	The average elemental composition (from two representative samples) of monazite and xenotime concentrate from <i>amang</i> 58
Table 6	Content of radionuclides related to <i>amang</i> sample, monazite and xenotime concentrate at <i>amang</i> processing plant in peninsular Malaysia. 75

LIST OF FIGURES

		Page
Figure 1	Map showing the global distribution of rare earth element deposits and mine (Walters, Lusty and Hill, 2011).....	8
Figure 2	Symmetry plane (left) and symmetry axis (right).	21
Figure 3	Axis of rotary-reflection (left) and symmetry center (right).	22
Figure 4	Monoclinic crystal axes.	25
Figure 5	Monoclinic prism and base (left) and clinodome and orthopinacoid (right).	26
Figure 6	Represents the combinations of monoclinic forms on crystal.....	26
Figure 7	Tetragonal crystal axes	27
Figure 8	Represents the first-order dipyramid (left), second-order dipyramid (middle) and ditetragonal dipyramid (right).....	28
Figure 9	Represents the combinations of tetragonal forms on crystal.....	28
Figure 10	A simplified flowchart illustrated the overall process to characterize the xenotime and monazite concentrate samples from Malaysian <i>amang</i>	32
Figure 11	Polished section of monazite (left) and xenotime (right).....	34
Figure 12	M4 Tornado for Micro-XRF analysis.	36
Figure 13	Graph of particle size distribution curve for both concentrate samples.	43
Figure 14	Monazite particle size fractions on (-425+250) μm , (-250+180) μm , (180+150) μm , (-150+125) μm , (-125+106) μm , (-106+90) μm , (-90+75) μm , (-75) μm and pan respectively.....	44
Figure 15	Xenotime particle size fractions on (-425+250) μm , (-250+180) μm , (-180+150) μm , (-150+125) μm , (-125+106) μm , (-106+90) μm , (-90+75) μm , (-75) μm and pan respectively.....	45

Figure 16	Graph of XRF analysis on monazite most retained particles at sieve 150µm, 180µm and 250µm.....	46
Figure 17	Graph of XRF analysis on xenotime most retained particles at sieve 125µm, 150µm and 180µm.....	47
Figure 18	Visual assessment of monazite (left) and xenotime (right) concentrate sample from Malaysian <i>amang</i> obtained for this project.....	48
Figure 19	Images from the optical microscope, monazite concentrate sample (left), and xenotime concentrate sample (right)	49
Figure 20	Photomicrograph on monazite crystal image under SEM Tabletop.	50
Figure 21	Photomicrographs of monazite crystal. (a,b)clearly prismatic crystal structure; (c)symmetry axis on monoclinic system	51
Figure 22	Image shows the characteristic combinations on monazite crystal. ..	51
Figure 23	Photomicrograph on xenotime crystal image under SEM Tabletop.	52
Figure 24	Photomicrographs of xenotime crystal. (a,b)clearly dipyramidal crystal structure (c)first-order dipyramid.....	53
Figure 25	Image shows the characteristic combinations on xenotime crystal...	53
Figure 26	SEM/EDX by selective area analysis on monazite mineral.....	54
Figure 27	The SEM/EDX spectra of monazite where elements are labelled on the peaks.....	55
Figure 28	SEM/EDX by selective area analysis on xenotime mineral.....	56
Figure 29	The SEM/EDX spectra of xenotime where elements are labelled on the peaks.....	57
Figure 30	A graph represents the weight percent of XRF analysis on the bulk chemical composition of monazite concentrate.	59
Figure 31	A graph represents the weight percent of XRF analysis on the bulk chemical composition of xenotime concentrate.	60

Figure 32	Spot area analysis (left) and distribution of main component on the monazite concentrate sample (right).....	61
Figure 33	Monazite concentrate sum spectrum (red) of the examined area normalized to the Rh-K-scatterer.	61
Figure 34	Element distribution of Al(a), Si(b), P(c), V(d), Cr(e), Fe(f), Y(g), Zr(h), U(i), Pb(j), La(k) and Nd(l) which are identified in the maximum pixel spectrum on the monazite concentrate sample.....	62
Figure 35	Spot area analysis (left) and distribution of main component on the xenotime concentrate sample (right).....	63
Figure 36	Xenotime concentrate sum spectrum (red) of the examined area normalized to the Rh-K-scatterer.	63
Figure 37	Element distribution of Al(a), P(b), Mn(c), Fe(d), Co(e), Ni(f), Y(g) and W(h) which are identified in the maximum pixel spectrum on the xenotime concentrate sample.....	64
Figure 38	A sample XRD pattern of the monazite concentrate from Malaysian amang.....	65
Figure 39	A sample XRD pattern of the xenotime concentrate from Malaysian amang.....	66
Figure 40	Moisture content test for both monazite and concentrate samples....	76
Figure 41	Sampling for both samples using cone and quartering method.....	76
Figure 42	Particle Size Distribution analysis by Electronic RX-29-10 sieve shaker.....	76
Figure 43	Scanning Electron Microscopy (SEM) using Tabletop Microscope SEM TM3030.....	76

LIST OF SYMBOLS

Bq	Becquerel; unit of radioactivity
kg	Kilogram
mSv h ⁻¹	Millisievert per hour; radiation dose rate
nGy h ⁻¹	Nano gray per hour; air absorbed dose rate
γ	Gamma

LIST OF ABBREVIATIONS

ANM	Malaysian Nuclear Agency
EDX	Energy Dispersive X-Ray
HREE	Heavy Rare Earth Element
LREE	Light Rare Earth Element
NORM	Naturally Occurring Radioactive Material
REEs	Rare Earth Elements
REO	Rare Earth Oxides
SEM	Scanning Electron Microscope
USM	Universiti Sains Malaysia
XRD	X-ray Diffraction
XRF	X-Ray Fluorescence

LIST OF APPENDICES

Appendix A

Appendix B

ABSTRAK

Amang, yang diiktiraf secara meluas untuk sisa buangan mineral di Malaysia, adalah produk sekunder sisa buangan-kasiterit atau oksida timah (SnO_2) yang terbentuk daripada proses pengasingan mineral seperti pemisah graviti, magnetik dan tegangan tinggi. Di Malaysia, unsur nadir bumi (REE) yang mengandungi monazit dan xenotime diperoleh daripada amang. Projek tahun akhir ini bertujuan untuk mencirikan mineralogi monazit dan xenotime daripada amang Malaysia. Mikroskop optik, dan mikroskop elektron pengimbasan (SEM) yang dilengkapi dengan sinar-X penyebaran tenaga (EDX) digunakan untuk penilaian morfologi bijih dan mineral berkaitan, serta analisis pembebasan mineral. Pendarfluor sinar-X (XRF) dan pembelauan sinar-X (XRD) digunakan untuk menentukan komposisi sampel monazite dan xenotime serta untuk mengenal pasti fasa mineral, masing-masing. Analisis XRF mengesahkan bahawa unsur-unsur dominan yang terdapat dalam sampel monazit ialah P dan Ce, diikuti oleh unsur-unsur yang terdapat dalam tahap surih seperti La, Nd dan Th. Untuk xenotime, yang menunjukkan jumlah Y dan P yang tinggi, dan juga mengandungi sejumlah besar LREE dan HREE. Analisis fasa oleh XRD pula mendedahkan monazite-(Ce) dan xenotime-(Y) sebagai komponen utama dalam kumpulan perwakilan monazit dan xenotime. Selain itu, analisis mineralogi bagi bahagian yang digilap telah dijalankan dan dianalisis di bawah mikroskop dan SEM/EDX. Imej SEM mendedahkan struktur kristal sampel monazit dan xenotime adalah dominan prismatic atau boleh dilihat sebagai kristal berbentuk baji dan dipyramidal, masing-masing. Penemuan menunjukkan bahawa morfologi, komposisi kimia dan jujuk fasa monazit dan xenotime telah dikenal pasti secara muktamad.

ABSTRACT

Amang, widely recognized for mineral tailings in Malaysia, is a cassiterite-tailing or tin oxide (SnO_2) secondary product inevitably formed from mineral separation processes such as gravitational, magnetic, and high-tensional separators. In Malaysia, rare-earth elements (REEs) bearing monazite and xenotime are recovered from *amang*. This paper aims to mineralogically characterize the monazite and xenotime concentrate from Malaysian *amang*. The optical microscope, and scanning electron microscope (SEM) equipped with an energy-dispersive X-ray (EDX) were used for ore morphology and mineral association assessment as well as mineral liberation analysis. X-ray fluorescence (XRF) and X-ray diffraction (XRD) were used to determine the monazite and xenotime concentrate sample composition and to identify mineral phases, respectively. XRF analysis confirmed that the dominant elements present in the sample monazite concentrate are P and Ce, followed by elements present in trace levels like La, Nd and Th. The xenotime concentrate, which indicated high amounts of Y and P, and also contained significant amounts of LREE and HREE. Phase analysis by XRD meanwhile revealed monazite-(Ce) and xenotime-(Y) as the major components in the monazite and xenotime representative group, respectively. Additionally, mineralogical analyses of polished sections were carried out and analysed under microscope and SEM/EDX. SEM images revealed the crystal structures of the monazite and xenotime concentrate samples are dominantly prismatic or can be seen as wedge-shaped crystals and dipyramidal, respectively. The findings demonstrated that the morphology, chemical composition and phase constituents of monazite and xenotime were conclusively identified.

CHAPTER 1 INTRODUCTION

1.1 Research Background

The higher tin production has resulted in the emergence of a new sector, tin by-product (*amang*) processing, to exploit mega tonnes of tin by-products created in the past. During Malaysia's tin rush, *Amang* was viewed as tailings and was deposited in large quantities, especially during the peak period of tin mining. *Amang* is made up of valuable rare-earth elements and multi-heavy minerals. After a few decades of rapid practice in mineral processing, it has been classified as a Technically Enhanced Naturally Occurring Radioactive Material (TENORM) (Sanusi et al., 2021).

The problem of environmental contamination caused by radioactive residues from the ^{238}U and ^{232}Th decay series, threatens to exacerbate the situation. Following the unresolved court case of Asian Rare Earth Sdn Bhd (ARE) radioactive *amang* pollution in Bukit Merah in 1982, the *amang* industry has been under pressure from both local and international sources (Sanusi et al., 2021). Uncontrolled and quick processing of *amang* causes symptoms such as shortness of breath and posing a significant risk of inhaling radioactive airborne dust among the locals.

Besides, due to a scarcity of tin resources in the late 1980s, the *amang* industry was forced to reduce its output and, in some cases, terminate operations, going from 81 processing units in 1984 to 66 in 1989 (Sulaiman et al., 1994). *Amang* minerals are projected to be constantly produced to some amount in the future, with a few significant factories remaining in Bukit Merah, Lembah Kinta (Ramli, 2007), Lembah Klang (Bahari et al., 2007), Kelian Intan (open-pit tin mining), and a few more in Johor and Pahang. In reality, the government has declared a full-scale restart of tin mining in 2019.

Now, *amang* has developed into a particularly interesting and potential mineral resource, as minerals like xenotime and monazite contain rare earth elements (REEs), which have become increasingly valuable. Xenotime and monazite are mostly distributed in placer deposits. Rare earth minerals are also found only in very fine grains, and physical separation procedures are ineffective for them. Around 60% of released monazite and xenotime in many deposits is smaller than 10 μ m, and only a few deposits, particularly placers, can have coarse-grained monazite and xenotime (Chan, 1992) which is difficult to recover in the beneficiation process.

Xenotime and monazite are known as rare earth phosphates where xenotime has natural heavy rare earth elements in the yttrium group (Ni et al., 1995) whereas monazite contains natural light rare earth elements in the cerium group and normally has large numbers of thorium and uranium (Clavier et al., 2011). They both sparked a lot of interest as viable options for a long-term energy supply. The heaviest naturally occurring elements on earth are thorium (Th) and uranium (U), however, in nature, the abundance of Th over U is highly limited. Using Th as a new primary source of nuclear energy has been a fascinating prospect for many years. However, overcoming the issue required a significant investment in research and development (Lainetti, 2015)

Th can be found in Malaysian minerals and rare earth elements in industrial waste. Several minerals in Malaysia, such as monazite, zircon, xenotime, and ilmenite, are classed as strategic minerals because they contain large amounts of Th and U exceeding 500 ppm, necessitating regulatory control. The average range of Malaysian monazite and xenotime minerals is at 70,000 and 15,000 ppm, respectively (Sulaiman, 1991). Although Th has the potential to pose a significant radioactive threat to our environment if not properly treated, its prospects as a future alternative fuel in nuclear technology are bright.

This paper explores the study of Malaysian rare earth elements of xenotime and monazite concentrate samples from Malaysian *amang*. This is done via physical characterization with the aid of mineralogical studies. In this study, two samples from *amang* indicate the concentrate of xenotime and monazite were obtained from the Malaysian Nuclear Agency (ANM) supplied by the Ipoh silica sands by Ooi Cheng Huat private limited company. This paper aspires to present a detailed vision and tell a fantastic story about monazite and xenotime as potential REE sources.

1.2 Problem Statements

Despite some understanding of rare earth elements environmental hazards when they are discharged into the environment alongside radionuclides, the widespread use of rare earth elements in many modern technologies continues to expand. The majority of the harmful effects of rare earth element exposure to humans and their potential health effects come from mine workers and others who work with rare earth elements. Also, their products are regularly, where exposure is typically much higher than what the general population would experience.

Concentrate from tin mining or cassiterite separation process contains unknown waste known as '*amang*' which cannot be identified whether its composition has economic value or not. *Amang* can be used for further re-processing to discover the rare earth elements in it. Nowadays, *amang* has developed into a particularly interesting and potential mineral resource, as minerals like xenotime and monazite contain rare earth elements.

Apart from that, the mineralogy study regarding this is less studied. Therefore, this project conducted a detailed study on the actual composition of *amang* which consists of monazite and xenotime minerals. Visual observation of both minerals is

not enough to identify the bulk chemical composition that is present in them. Instead, it is also impractical to study the minerals present in both without further characterization. Thus, there are concentrate samples of monazite and xenotime from *amang* that will be carried out to be characterized in this project.

1.3 Research Objectives

1. To determine the bulk chemical composition of the concentrate sample.
2. To identify the morphology of the monazite and xenotime mineral.
3. To determine the mineral characterization of monazite and xenotime concentrate sample by particle size distribution, elemental composition using XRF, phase identification using XRD, mineral identification and microscopy study using SEM, and ore microscopy.

CHAPTER 2 LITERATURE REVIEW

2.1 Introduction

This chapter evaluates the literature review starting from the *amang*, which is where the origin of the samples comes from, and the story of the rare-earth elements (REEs) and REE-bearing minerals of monazite and xenotime. A detailed discussion on the particle size distribution, moisture content test, X-Ray Fluorescence (XRF), Micro X-Ray Fluorescence (Micro-XRF), X-Ray Diffraction (XRD), ore microscopy, Scanning Electron Microscopy (SEM), and Scanning Electron Microscopy/Energy Dispersive X-Ray (SEM/EDX) are being reviewed for characterization of monazite and xenotime towards a better understanding. In addition, the literature review also has an eye on the crystallography of monazite and xenotime.

2.2 Amang

Amang, widely recognized for mineral tailings in Malaysia, is a cassiterite-tailing or tin oxide (SnO₂) secondary product inevitably formed from mineral separation processes such as gravitational, magnetic, and high-tensional separators. In Malaysia, rare-earth elements (REEs) bearing monazite and xenotime are recovered from *amang*. The *amang* were left since not many people knew their uses. Nowadays, *amang* is becoming more important since we can recover valuable heavy minerals from it. Accumulation of *amang* generates significant economic interest due to the high amount of valuable minerals.

Knowing that *amang* is made up of valuable rare-earth elements and multi-heavy minerals. *Amang* poses an extremely high radioactivity problem associated with high occupational ionizing radiation exposures to workers and continuously impacts the local environment with radioactive contamination from industrial effluent and solid waste into the lithosphere and water bodies. This is basically due to poor safety and health practices in such operating plants.

The issue of high radioactivity related to significant occupational ionizing radiation exposures has sparked an ongoing debate in the *amang* processing industry (Saito and Jacob, 1995, UNSCEAR, 2008). For instance, elevated radioactivity concentrations detected for ^{238}U and ^{232}Th decay nuclides could be as high as 200,000 and 400,000 Bq kg⁻¹, respectively. Such an amount could yield more than 30,000 nGy h⁻¹ of gamma (γ) radiation exposure (Sanusi et al, 2021). Any attempt by *amang* operators to manage and handle *amang* products could expose them to relatively high γ equivalent doses exceeding 100 mSv h⁻¹.

In earlier decades in the 1980s and 1990s when the industry was at its peak, significant proportion of sources regarding radionuclides were reported. The majority of essential data are retrieved from internal and unpublished reports from a government department and regulatory body libraries such as the Department of Geological Survey, Southeast Asia Tin Research and Development Centre, Malaysia Nuclear Agency (ANM), and Atomic Energy Licensing Board of Malaysia. Thus, the content of radionuclides related to *amang* sample, monazite, and xenotime concentrate at the *amang* processing plant in Peninsular Malaysia is listed in Appendix A.

2.3 Rare Earth Elements (REEs)

Due to the resemblance in the physical and chemical properties of gangue minerals and rare-earth elements, as well as the difficulty in locating concentrated deposits, these elements are referred to as "rare" due to the difficulties in extracting them from deposits. The heterogeneity of these elements in deposits, which influences the geology, adaptability, and composition of the minerals, adds another challenge to the production of rare earth elements (Gupta et al., 2004). Until recently, relatively only a few people, such as chemists, geologists, and specialized materials and technology engineers, were familiar with REEs.

REEs are very valuable and have high demands for advanced technology nowadays. It has become immensely significant in our world of technology because of its distinctive magnetic, phosphorescent, and catalytic capabilities. Cell phones and televisions, as well as LED light bulbs and wind turbines, all rely on these elements. Besides, there is fast growth in new applications and demand for rare earth elements, especially in energy, environment, and high technology fields with durability, high efficiency, and low carbon emissions (Alami et al., 2013).

The global production of REEs and the global reserves suggest that REE extraction is restricted to a few geographical concentrations in a few nations. Even though REE deposits can be found all over the world, the majority of the current global supply comes from operating mines in China. The Chinese have dominated the rare earth supply chain over the years. World production is relatively small and almost entirely comes from China (Walters, Lusty, and Hill, 2011).

However, in recent years, due to several circumstances, China's production has slightly dropped. The map below shows the global distribution of rare earth element deposits and mines (Figure 1). For some deposits, for instance, the CREE-rich Bear Lodge, which began operations in 2016, is one of the most interesting rare earth deposits in the United States. Zandkopsdrift, also in South Africa, is thought to be one of the world's largest REE deposits outside of China (Barakos et al., 2015).

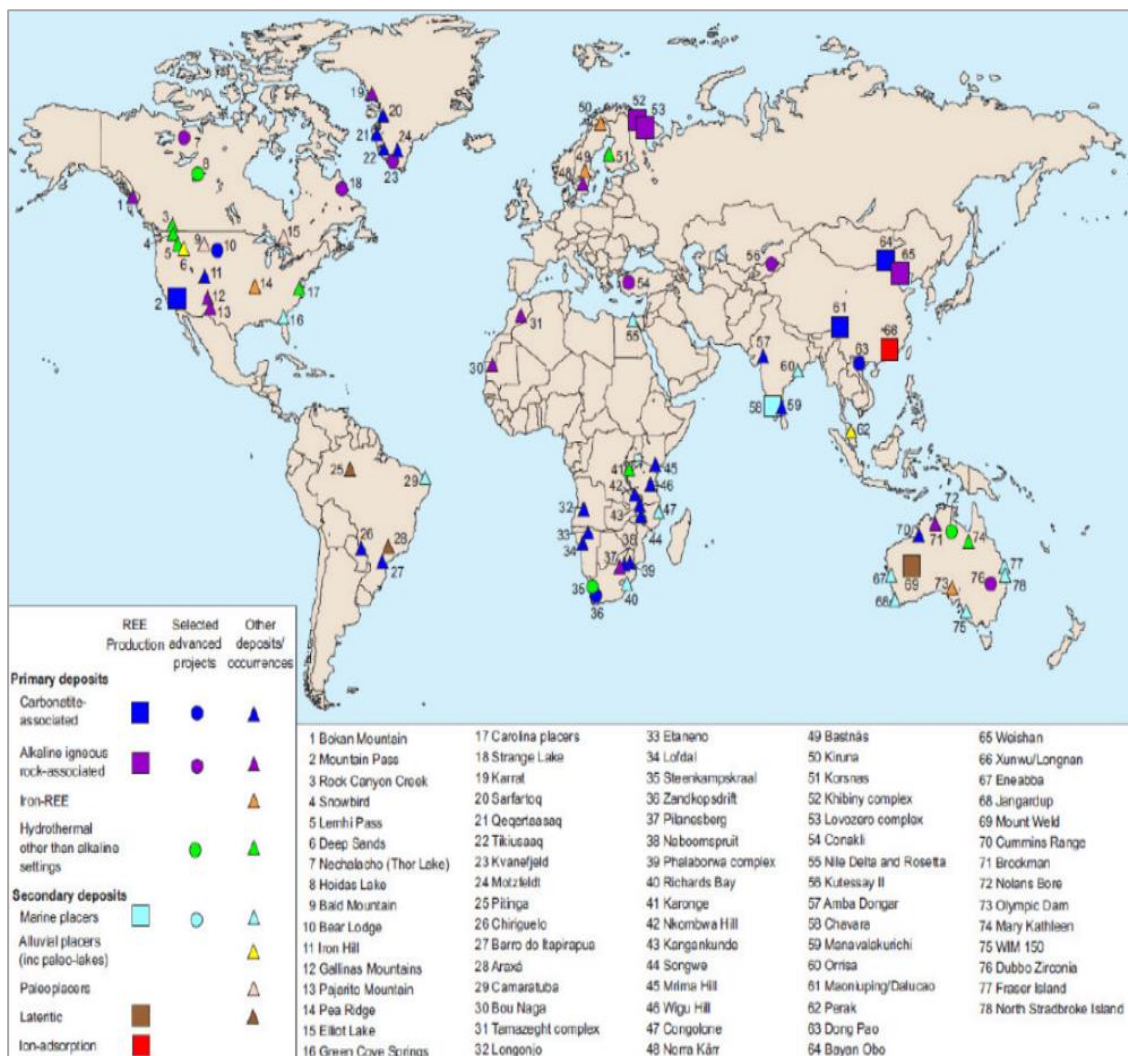


Figure 1 Map showing the global distribution of rare earth element deposits and mine (Walters, Lusty and Hill, 2011).

2.4 Monazite

Monazite [(Ce, La,Nd, Th)PO₄] is derived from the Greek verb ‘monazein’, which meaning ‘to be alone’. It is a relevant name as it describes the typical crystal habit of primary origin for monazite as an isolated individual crystal in phosphatic and pegmatites. Common minerals associated with are quartz, microcline, albite, muscovite, biotite, columbite, zircon, anatase, xenotime, and samarskite. It is normally transparent to translucent. Monazite shades of brown to reddish and yellowish-brown, also may appear in yellow, orange, and pink while the streak appears in white. The specific gravity and cleavage, respectively, are 4.6 to 5.7 and 2,2 which may exhibit parting. The Mohs hardness is about 5.0 to 5.5. The luster and tenacity of xenotime are resinous and brittle, respectively. Besides, the fracture can be conchoidal and uneven. Monazite commonly found as prismatic or wedge-shaped crystal and having paramagnetic, moderately and strongly behaviour.

Monazite is known as a primary ore of several rare earth metals most notably thorium, cerium, and lanthanum. All of these metals have a variety of industrial applications and are considered valuable. Thorium is a highly radioactive metal and could be used as a replacement for uranium in nuclear power generation. Besides, it can be used in refractory applications, lamp mantles, aerospace alloys and welding electrodes. Cerium can be used as a catalytic converter for the oxidation of CO emissions in the exhaust gasses from motor vehicles.

Monazite is a reddish-brown phosphate mineral that contains rare-earth elements. Because of the presence of thorium and, less commonly, uranium, it is radioactive. Monazite geochronology uses the radiogenic decay of uranium and thorium lead to be dated through monazite geochronology. Monazite is an accessory mineral found in igneous, metamorphic, and sedimentary rocks.

2.5 Xenotime

Xenotime (YPO_4) has been derived from the Greek word 'xeons' and 'time', which means 'foreign' and 'honor' respectively. Xenotime has traces of arsenic, silicon dioxide, and calcium impurities and joins in a solid solution series with chernovite. The main component of the rare-earth phosphate mineral xenotime is yttrium orthophosphate (YPO_4). Common minerals associated with are quartz, microcline, albite, rutile, muscovite, biotite, zircon, anatase, monazite. It is normally translucent to opaque but transparent in microcrystal. Xenotime shades of brown to brownish-yellow but also reddish to greenish-brown and grey, while the streak appears either in white, light yellow, or light brown color. The specific gravity is 4.4 to 5.11. The Mohs hardness is about 4 to 5. The luster of xenotime is vitreous and resinous, while the fracture and tenacity of xenotime are splintery and brittle, respectively.

Xenotime is a yttrium source. The most common applications of yttrium in phosphor powders for low-energy lighting. Yttrium is also employed in the production of yttrium-aluminum garnet lasers and yttrium iron garnet microwave filters. It's also utilized to make cubic zirconia diamonds, fighter jet engines, medicinal and graphic technology, and electronic components for missile defense systems.

Xenotime is a minor accessory mineral found in pegmatites and other igneous rocks, as well as gneisses rich in mica and quartz. The rare-earth elements dysprosium, erbium, terbium, and ytterbium, as well as metal elements such as thorium and uranium, are the most expressive secondary components of xenotime. Due to uranium and thorium impurities, certain xenotime may be moderate to severely radioactive (Webster, R., 2000).

2.6 Characterization of Monazite and Xenotime

Sample characterization involves the study of samples in terms of their size, chemical composition, phase identification, morphology, and other attributes. Therefore, particle size analysis, XRF, micro-XRF, XRD, SEM-EDX, optical microscope analysis are performed to learn more about the particle size distribution, mineral composition and identification on the concentrate sample.

2.6.1 Particle Size Analysis

Particle size analysis is the fundamental section of laboratory testing to study the liberation size of minerals. It shows ranges of size in a minerals sample. This analysis was conducted to obtain data for particle size distribution in the concentrate samples. The particle size distribution gradient will determine the distribution pattern in a sample. A steep gradient indicates a small size range of mineral samples or called single size. Then, the less steep gradient in particle size distribution shows minerals varied with size range.

Sieving analysis is done to obtain the particle size distribution. During sieving, the particles are compared with the apertures of every single sieve. The probability of a particle passing through the sieve mesh is determined by the ratio of the particle size to the sieve openings, the orientation of the particle, and the number of encounters between the particle and the mesh openings. The results of sieving analysis are generally presented by semi-logarithmic plots known as particle size distribution curves. The particle diameters are plotted in log scale, and the corresponding percent finer in arithmetic scale.

In addition, the value of percentiles in the graph will indicate the statistic of the size distribution of a sample. It provides information on how the size distribution is spread over the interval from smaller value to largest value. The D_{75} , D_{50} , D_{25} values represent the 75th, 50th and 25th percentile of cumulative passing size respectively. The 75th percentile is known as third quartile, 50th percentile as the median and 25th percentile as first quartile.

Uniformity coefficient, C_u can be calculated to determine the gradation of the sample. If the C_u value is more than 6, means the sample is well graded. Sample contains particles of a wide range of sizes and has a good representation of all sizes. If the C_u value is less than 6, means the sample does not have a good representation of all sizes of particles. Sample mostly has single-size particles (Holtz and R., 1981).

$$C_u = \frac{D_{60}}{D_{10}} \quad (\text{Equation 1})$$

Where

D_{10} = passing size of mineral at 10%

D_{60} = passing size of mineral at 60%

2.6.2 Moisture content

The moisture content of concentrate sample, also known as water content, is a measure of how much water is actually present in the concentrate. The ratio of the mass of water to the mass of solids in a sample, stated as a percentage, is what is meant by the term "moisture content." In equation form,

$$w = \frac{M_w}{M_s} \times 100 \quad (\text{Equation 2})$$

Where

w = moisture content of concentrate

M_w = mass of water in concentrate sample

M_s = mass of concentrate solids in sample

It should be noted that the moisture content may be incorrectly defined as the proportion of water mass to the total mass of moist concentrate rather than to the mass of oven-dried concentrate. This incorrect definition would result in a fraction in which both the numerator and denominator vary depending on the amount of moisture present, but not in the same proportion because the total mass of moist concentrate is the sum of the mass of water and oven-dried concentrate. Such a definition would not be desirable because moisture content would then be determined by the amount of moist mass of concentrate, which would vary, as opposed to the amount of oven-dried concentrate, which would remain constant. Or, to put it another way, the moisture content would not be directly proportional to the mass of water present if the definition were incorrect.

2.6.3 X-Ray Fluorescence (XRF)

XRF is a non-destructive analytical technique used to determine the major and trace elements in the samples. XRF analyzers determine the chemistry of a sample by measuring the fluorescent or secondary X-ray emitted from it when excited by a primary X-ray source. Each element in a sample emits a distinct set of fluorescent X-rays, or "fingerprint," that is unique to that element, which is why XRF spectroscopy is such an effective tool for qualitative and quantitative material composition analysis.

There are two types of XRF which are Energy dispersive spectrometers (EDS) and wavelength dispersive spectrometers (WDS). Energy dispersive spectrometers (EDS) sort the X-rays based on their energy while wavelength dispersive spectrometers (WDS) sort the X-rays based on their wavelengths. Either one of the methods can be used for the sample analysis. The high energy of X-ray will bombard from the source and excites the atoms in a sample. Photons will be emitted from the surface of the sample and detected by the detector. The data collection and processing system will identify the presence of minerals in a sample (Leng, 2010).

2.6.4 Micro X-Ray Fluorescence (Micro-XRF)

Micro-XRF is the tool of choice for small-spot sample characterization using an energy-dispersive method that guides excitation X-rays into a micrometer-sized spot on the sample along with high X-Ray intensity by a polycapillary lens. Even from below the surface, its measurements provide information about composition and element distribution. The micro-XRF spectrometer is optimized for speed analysis of points, lines, and 2D area scans which is also called element mapping. As a result, it can tell you not only what elements are in a sample and how much of them, but also where they are in the sample.

This method is ideal for measuring and understanding inhomogeneous samples, especially when combined with a fast-scanning stage. Almost any sample can be measured using micro-XRF includes solids, powders, and liquids. Sample preparation is very minimal, and the sample is not damaged during the measurement process, as is the case with all XRF methods. Not only in forensics, but also in other fields, micro-XRF is an excellent pre-screening technique.

In the post-processing, it is possible to examine the spectrum of each pixel or combine the spectra of several pixels to improve the counting statistics instead to generate distributions for each energy range, either for elements that are in the examined sample, for the entire energy range, or also for unique background energies. Also, to calculate the artificial maximum pixel spectrum, which contains for each channel the channel's highest intensity of the entire mapping (Haschke et. al, 2022). This makes it possible to identify hotspots in the sample as well as to assess the linear distribution of each line in the mapping.

2.6.5 X-Ray Diffraction (XRD)

XRD is a technique employed to determine the underlying crystal structure of a material, it enables verification of the crystallinity and structure of a sample but gives no information of a chemical nature. Fitting XRD patterns can allow the calculation of the material lattice parameters, the orientation of a crystal or grain, the stress in crystalline regions, and secondary phases in the sample (Fleck, 2021). It is generally a bulk characterization technique and produces an average diffraction pattern for the area measured. XRD is a non-destructive technique that can be conducted at room temperature and pressure.

X-rays are electromagnetic waves with high frequency and short wavelength. In an X-ray tube, the filament is heated to produce electrons. The high voltage in the X-ray tube allows the electrons to accelerate toward the target in vacuum. Therefore, high-speed electrons are bombarded to a target with high energy. X-rays are produced after the collision of high-speed electrons with the target. Electron of an atom's inner shell will be excited when it has sufficient energy. Transition of electrons will occur.

Electrons jump from lower to higher energy levels. As the electron falls, energy will be released by emitting photons with specific energy. In other words, X-ray with specific wavelengths is produced. The wavelength is analyzed and interpreted by the system.

From the Bragg's Law equation, $n\lambda = 2d \sin\theta$, the information on the spacing between atomic planes of a crystal can be obtained when constructive interference is detected at a given incident angle and a wavelength of the incident beam. The incident ray must be travel in phase. When the spacing between atomic planes is obtained, crystal structure of a materials can be determined (Leng, 2010).

2.6.6 Ore Microscopy

The ore microscope is the basic instrument for the petrographic examination of the large and economically important group of minerals referred to collectively as ore or opaque minerals. The ore microscope has systems of lenses, polarizers, analyzers, and different diaphragms similar to those used in conventional petrographic microscopes, but it differs in that its main source of illumination is an overhead light source that enables analysis of light reflected from polished surfaces.

The increasing interest in ore-gangue relationships and the recognition that much textural information can be derived from the examination of translucent ore minerals in polished thin sections, now commonly leads to the use of microscopes equipped for both reflected and transmitted light study (James, 1994). Qualitative optical characteristics such as the colour, shape and mineral association were distinguished by reflected light microscope. Microscopic studies on different areas in the same sample revealed different mineral associations.

Observations with an ore microscope are usually made either with Plain Polarized Light (PPL) or with Crossed Polarized Light (XPL). During the observation with PPL, a mineral can be determined by its colour, hardness, reflection pleochroism and reflectance birefractance while XPL, anisotropism and internal reflections can be observed. Isotropic and anisotropic minerals are most of the time easily distinguished because isotropic minerals do not transmit light which is always black when viewed under XPL.

2.6.7 Scanning Electron Microscopy (SEM)

Scanning Electron Microscope can be used for imaging and microscopic analysis of biological, inorganic, and man-made materials. All scanning electron microscopes utilise a focused beam of electrons to scan the surface of a sample to create a high-resolution image or 3-dimensional image. SEM generates images that provide details about a material's surface composition and topography. The only utilities needed are a small, quiet roughing vacuum pump and normal AC electricity. There is no need for additional cooling, air conditioning, or foundation. Due to ambient conditions in some situations, a vibration isolation table or support could be advised when users want to reach the greatest magnifications.

SEM produces enlarged, fine-grained pictures of an object by scanning a focused beam of electrons. It produces an image by detecting reflected or knocked-off electrons. An electron gun accelerates the microscope as it emits electrons, which go through a sequence of lenses and apertures to create a focused beam that eventually interacts with a sample's surface.

After the sample is set up on a stage inside the microscope chamber, a succession of pumps create a vacuum inside the space. The vacuum level is determined by the design of the microscopes, thus the chamber doesn't need to be evacuated.

The location of the electron beam above the objective lens is controlled by scan coils. These coils enable the beam to scan across the sample's surface while gathering information about a particular region. Different signals, such as secondary electrons, backscattered electrons, and distinctive X-rays, are produced by the interaction of the sample and the electron and are picked up by detectors. The images produced by these detectors are then produced and shown on a computer screen.

2.6.8 Scanning Electron Microscopy(SEM)/ Energy Dispersive X-Ray(EDX)

Scanning Electron Microscopy (SEM) with energy dispersive X-Ray (EDX) is used to study the liberation size of the mineral. The scanning electron microscope (SEM) produces a variety of signals at the surface of solid specimens using a focussed beam of high-energy electrons. The signals produced by electron-sample interactions include details about the exterior morphology, texture, chemical composition, crystalline structure and orientation of the constituent materials on the samples (Moecher and David, 2004).

The most frequent SEM mode is the detection of secondary electrons given off by excited atoms. A high-resolution image exhibiting the topography of the surface is produced by scanning the sample and collecting the secondary electrons that are emitted using a special detector. In a SEM equipped with EDX spectroscopy, distinctive X-rays generated by the interaction of electrons with the sample can also be discovered. The composition and elemental abundance of the sample are determined through analysis of the x-ray emissions.

The areas of liberated and locked particles (representatively sampled) were assessed and the total areas were estimated and calculated, effectively yielding the degree of liberation. As reported by Olubambi (Olubambi et. al, 2008), the degree of liberation is defined by the equation,

$$\% \text{ Mineral Liberation} = \frac{FM}{FM + LM} \times 100 \quad (\text{Equation 3})$$

Where,

FM = Total area of mineral particles (of interest) liberated

LM = Total area of mineral particles (of interest) interlock

2.7 Crystallography

The vast majority of minerals, crystals are distinct geometrical structures that form when the conditions are right for their formation. The study of these structures and the laws governing their development, morphology, and geometrical character is known as crystallography. Despite having started out as a subfield of mineralogy, crystallography has since grown to the point where it is now considered to be a distinct field of study. Therefore, a volume much larger than the one we're using now would be necessary to discuss in detail.

The elements of crystallography are briefly and simply described in the following section to expose the reader to the more crucial facts and concepts of the topic. A crystal is a homogenous entity surrounded by smooth plane surfaces that externally expresses an organized internal atomic structure. There is a growing tendency to refer to any solid that has a definite atomic structure as a crystal, regardless of whether it has external faces, especially among physicists.

It seems preferable to use the term "crystal" in the restricted sense as described above because such usage is contrary to the beliefs of the majority of mineralogists and necessitates the use of modifiers. The word "crystal" primarily refers to the faces of the crystalline substance. The term "crystalline" is a general one that denotes the orderly arrangement of atoms in the structure. Crystals with such fine grains are referred to as "cryptocrystalline," and only a microscope can clearly see their crystal structure. When an object's ordered atomic structure is completely missing, the object is said to be amorphous.

All crystals have a certain symmetry in the arrangement of their faces, which enables classification into different types. The various operations that can be performed on a crystal to cause it to coincide with the initial position are known as the elements of symmetry. The three fundamental symmetry operations are rotation about an axis, reflection in a plane, and rotational reflection, which combines rotation about an axis with reflection in a plane perpendicular to the axis.

A symmetry plane is a theoretical plane that divides a crystal into two halves, each of which is a fully formed crystal and is the mirror image of the other. An imaginary axis that traverses a crystal and permits at least two full rotations of the crystal around it is known as a symmetry axis.

The crystal seen in Figure 2 below will appear the same when rotated 180 degrees about the line C-C'. In other words, the lines C-C' become an axis of symmetry since analogous planes, edges, and solid angles will show up where their corresponding counterparts did in the initial position. Points A' and B' will take up the original positions of points A and B, respectively.

As a result of the crystal appearing twice throughout a complete revolution, this axis is known as possessing 2-fold or binary symmetry. Along with axes of 2-fold symmetry, there are also axes of 3-fold (trigonal), 4-fold (tetragonal), and 6-fold (hexagonal) symmetry. Because of the nature of crystals, only the 2-, 3-, 4-, and 6-fold axes can exist.

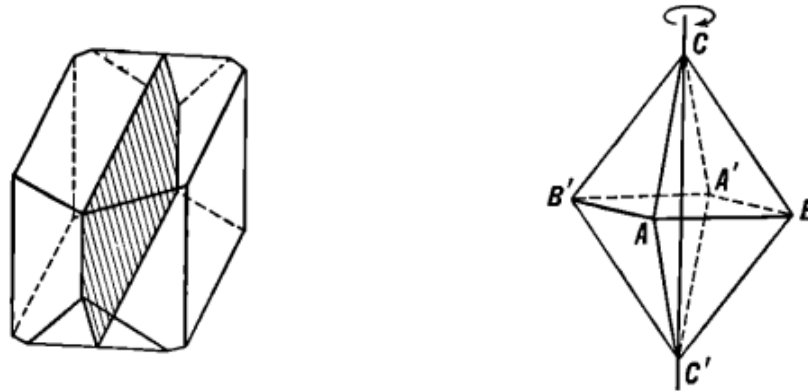


Figure 2 Symmetry plane (left) and symmetry axis (right).

This composite symmetry element, known as the axis of rotary reflection, combines rotation about an axis with reflection across a plane at an angle to the axis. Before obtaining the new position, both requirements must be completed. Figure 3 depicts the two-fold axis of rotating reflection. The solid point p' can be obtained by rotating the axis by 180° and reflecting it in the plane m . Figure 3 also depicts a crystal with a dual axis of rotating reflection. A crystal is said to have a centre of symmetry if an imaginary line can be formed through any point on its surface and terminates at the centre, and if another point along the line can be located at an equal distance from the centre. Because the point A is replicated at A' on the line joining A and the crystal's centre, C , the distances AC and $A'C$ are equal, and as a result, the crystal in Figure 3 has a centre of symmetry.

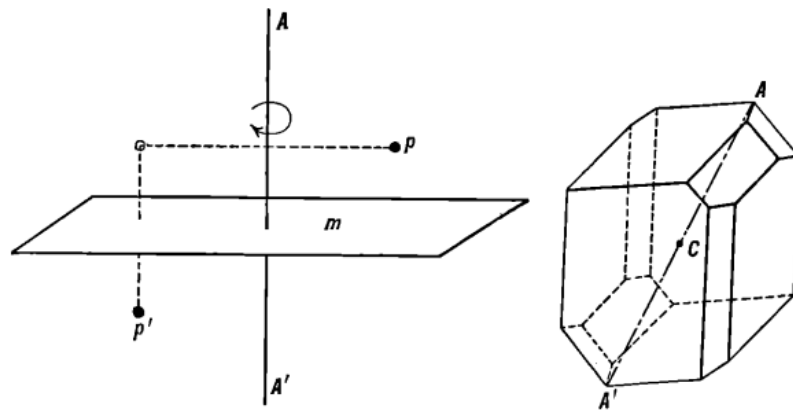


Figure 3 Axis of rotary-reflection (left) and symmetry center (right).

An axis of rotating reflection is indicated by A_n in symmetry notation, where n may be 2, 3, 4, or 6 depending on the symmetry of a plane (P) and a centre (C). A crystal having a centre, four 2-fold axes, one 4-fold axis, and five planes would have the following spelled out in its symmetry: $C; 4A_2, 1A_4; 5P$.

Additionally, the term "crystal habit" describes the typical and characteristic form (or mixture of forms) in which a material crystallises. If crystal growth irregularities are significant, it also considers their general distribution and shape. There is limited information on the factors that influence habit, but it is thought that temperature, pressure, crystal growth rate, and solution type all play a role.

The various symmetry elements can be combined to generate 32 different crystal classes. Theoretical analysis has shown that these encompass all potential crystal symmetry classes, which are further subdivided into six systems. The majority of the 32 possible crystal classes are of little interest to mineralogists because almost all known mineral species may be grouped into one of ten or twelve groups. The Table 1 on page 23 lists all of the crystal classes and the symmetry elements.

Table 1 All of the 32 crystal system and classes with their symmetry components.

Crystal System	Crystal Class	Symmetry
Isometric	Hexoctahedral	$C, 3A_4, 4A_3, 6A_2, 9P$
	Gyroidal	$3A_4, 4A_3, 6A_2$
	Hextetrahedral	$3A_2, 4A_3, 6P$
	Diploidal	$C, 3A_2, 4A_3, 3P$
Hexagonal Hexagonal division	Tetartoidal	$3A_2, 4A_3$
	Dihexagonal-dipyramidal	$C, 1A_6, 6A_2, 7P$
	Hexagonal-trapezohedral	$1A_6, 6A_2$
	Dihexagonal-pyramidal	$1A_6, 6P$
	Ditrigonal-dipyramidal	$1A_3, 3A_2, 4P$
	Hexagonal-dipyramidal	$C, 1A_6, 1P$
Hexagonal Rhombohedral division	Hexagonal-pyramidal	$1A_6$
	Trigonal-dipyramidal	$1A_3, 1P$
	Hexagonal-scalenohedral	$C, 1A_3, 3A_2, 5P$
	Trigonal-trapezohedral	$1A_4, 3A_2$
	Ditrigonal-pyramidal	$1A_3, 3P$
Tetragonal	Rhombohedral	$C, 1A_3$
	Trigonal-pyramidal	$1A_3$
	Ditetragonal-dipyramidal	$C, 1A_4, 4A_2, 5P$
	Tetragonal-trapezohedral	$1A_4, 4A_2$
	Ditetragonal-pyramidal	$1A_4, 4P$
	Tetragonal-scalenohedral	$3A_2, 2P$
	Tetragonal-dipyramidal	$C, 1A_4, 1P$
Orthorhombic	Tetragonal-pyramidal	$1A_4$
	Tetragonal-disphenoidal	$1A_4$
	Rhombic-dipyramidal	$C, 3A_2, 3P$
Monoclinic	Rhombic-disphenoidal	$3A_2$
	Rhombic-pyramidal	$1A_2, 2P$
	Prismatic	$C, 1A_2, 1P$
Triclinic	Sphenoidal	$1A_2$
	Domatic	$1P$
Triclinic	Pinacoidal	C
	Pedial	<i>No symmetry</i>

The crystallographic axes are used to define the six crystal systems. All crystals that can be described by three axes that are perpendicular to one another and have equal lengths are said to be in the isometric system. All crystal systems with four axes are referred to as hexagonal systems. A fourth horizontal axis, which is of varied length and perpendicular to the plane of the other three, intersects three equal horizontal axes at angles of 60° . All crystals with three mutually perpendicular axes, two horizontal axes of equal length, and a vertical axis that is either shorter than or longer than the other two are referred to as having the tetragonal system. All crystals that are identified by three axes that are mutually perpendicular and all have different lengths belong to the orthorhombic system. All crystals having three uneven axes, two of which are obliquely inclined to one another and the third is perpendicular to the plane of the other two, are referred to as belonging to the monoclinic system. All crystals having three uneven axes that all cross at acute angles are said to have a triclinic system.

2.7.1 Monazite

Monazite is a prismatic mineral with a monoclinic crystal structure. In the monoclinic system, there are three crystallographic axes with various lengths. While axes a and c form some oblique angles with one another, axes a, b, and c form 90° angles with one another. The axes' relative lengths and the angle between the a and c axes for each monoclinic mineral must be determined using the accurate dimensions. When it is properly oriented, the ortho-axis, also known as b, is horizontal and parallel to the observer. The clino-axis, also known as a, is vertical, while c is perpendicular to the observer.